Electronic Supplementary Information

Improving the charge transport of the ternary blend active layer for efficient semitransparent organic solar cells

Pan Yin,[ab] *Zhigang Yin,*[a] *Yunlong Ma*[a] *and Qingdong Zheng**[a]

[a] State Key Laboratory of Structural Chemistry, Fujian Institute of Research on the Structure of Matter, Chinese Academy of Sciences, 155 Yangqiao Road West, Fuzhou, 350002, China. E-mail: qingdongzheng@fjirsm.ac.cn.

[b] University of Chinese Academy of Sciences, 19 Yuquan Road, Beijing, 100049, China.

Experimental section

Materials: PBDB-TF, Y6 and other materials used in this work were purchased from Solarmer Energy Inc, Sigma-Aldrich, Alfa Aesar, Adamas-beta Ltd and Suna Tech Inc. Unless otherwise specified, these materials and chemicals were used without any further purification. The synthesis of DTNIF has been reported by our group previously.[S1]

General Characterization: UV-Vis absorption spectra and transmittance spectra were measured on a PerkinElmer Lambda 365 spectrometer. The PL spectra were conducted on an Edinburgh Instrument FLS 920. Surface morphologies of the active layers were analyzed using a dimension icon AFM in the tapping mode. GIWAXS measurements were performed at 13A beamline of National Synchrotron Radiation Research Center (NSRRC, Taiwan). Ceshigo Research Service (www.ceshigo.com) provided the technical support for the GIWAXS measurements. The GIWAXS samples were prepared on PEDOT:PSS-coated Si substrates using the identical blend solutions as those for the best-performance OSCs. All samples for the GIWAXS measurements were radiated at 12.13 keV X-ray with an incident angle of 0.10-0.15°. The coherence

length was estimated by the Scherrer equation: CL = 2πK/FWHM, where FWHM is the full width at half-maximum of the peak and K is a shape factor (0.9 was used here).

Device Fabrication and Characterization: Devices with a conventional structure of ITO/PEDOT:PSS/active layer/PDIN/Ag were fabricated in a glovebox, where the active layer was comprised of the binary or ternary blends with PBDB-TF, Y6 and/or DTNIF. The ITO patterned glass was cleaned with ultrasonic treatment in detergent, deionized water, acetone, ethanol, and isopropyl alcohol sequentially, and dried in an ultraviolet–ozone chamber for 15 min. The PEDOT:PSS layer was deposited by spin-coating at 3500 rpm on top of the pre-cleaned ITO glass substrate. The binary and ternary blends were pre-dissolved in chloroform with different weight ratios using 1-chloronaphthalene (0.5% volume) as the solvent additive. The mixed solutions were spin-coated onto the PEDOT:PSS-covered substrates at 4000 rpm for 50 s, and the resulting active layers were annealed at 90 °C for 5 min. Then the PDIN solution was spin-coated onto the active layers at 4000 rpm for 30 s. Finally, ~100 nm of Ag was deposited on the PDIN layer through shadow masks (0.04 cm^2) by thermal evaporation. The thicknesses of the active layer were controlled by varying the spin-coating speed and blend concentration, and measured on a Bruker Dektak XT surface profilometer. Photovoltaic performance of solar cells was tested under 1 sun, AM 1.5G spectrum (100 mW cm^{-2}) from an Oriel sol3A solar simulator (Newport). *J-V* measurements were carried out using a Keithley 2400 source meter. The light intensity for *J-V* measurements was calibrated with a NREL-certified silicon reference cell. EQE data were taken using the QE/IPCE measurement kit (QE-PV-SI) from Newport.

Fabrication and Characterization of Hole- and Electron-Only Devices

The charge transport properties were evaluated by the SCLC method with a hole-only device configuration (ITO/PEDOT:PSS/active layer/MoO_3/Ag) for hole mobility, and an electron-only device configuration (ITO/ZnO/active layer/Ca/Al) for electron mobility, respectively. Hole- and electron-only devices were fabricated under the similar fabrication condition for the best-performance ternary devices. The thickness of

the film was measured by a Bruker Dektak XT surface profilometer. The *J-V* characterization of the devices was measured by using a computer controlled Keithley 2440 source meter. Both hole and electron mobilities were extracted by fitting the *J-V* curves using the empirical Mott–Gurney formula in single carrier SCLC device using the following equation:[S2-S3]

$J = \frac{9}{8}\varepsilon_r \varepsilon_0 \mu \frac{V^2}{L^3}$, where ε_r is the relative dielectric constant of the active layer material (assumed to be 3), μ is the hole or electron mobility, ε_0 is the permittivity of empty space (8.85×10^{-12} F m^{-1}), L is the film thickness of the active layer, V is the internal voltage in the device, and $V = V_{appl} - V_{bi}$, where V_{appl} is the applied voltage to the device, and V_{bi} is the built-in voltage due to the relative work function difference between the two electrodes (in the hole- and electron-only devices, the V_{bi} values are 0.2 and 0.7 V, respectively), and J is the current density (A m^{-2}).

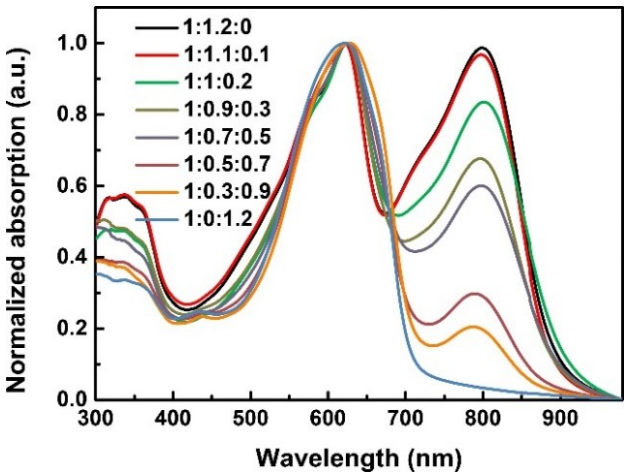

Figure S1. Normalized absorption spectra of PBDB-TF:Y6:DTNIF blend films with different weight ratios.

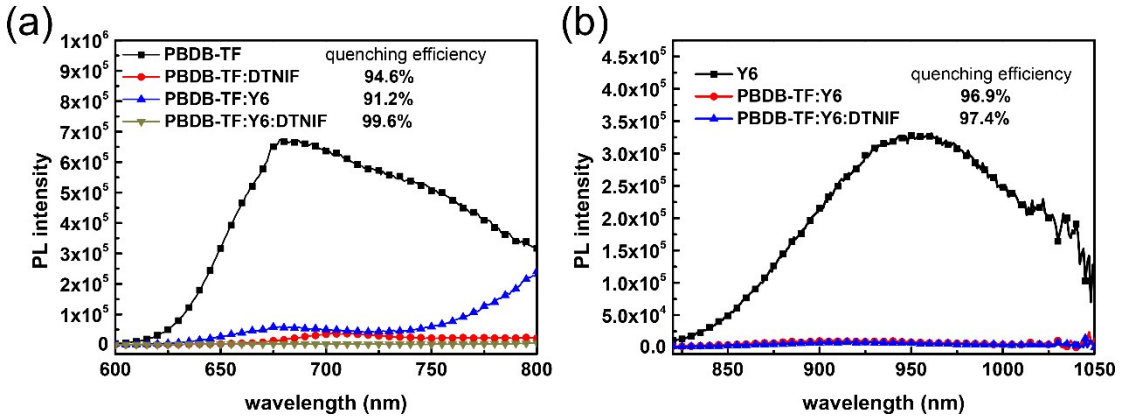

Figure S2. a) PL spectra of the neat PBDB-TF film, binary PBDB-TF:DTNIF blend film, binary PBDB-TF:Y6 blend film, and ternary PBDB-TF:Y6:DTNIF (1:1.1:0.1) blend film upon an excitation at 580 nm. b) PL spectra of the neat Y6 film, binary PBDB-TF:Y6 blend film, and ternary PBDB-TF:Y6:DTNIF (1:1.1:0.1) blend film upon an excitation at 800 nm.

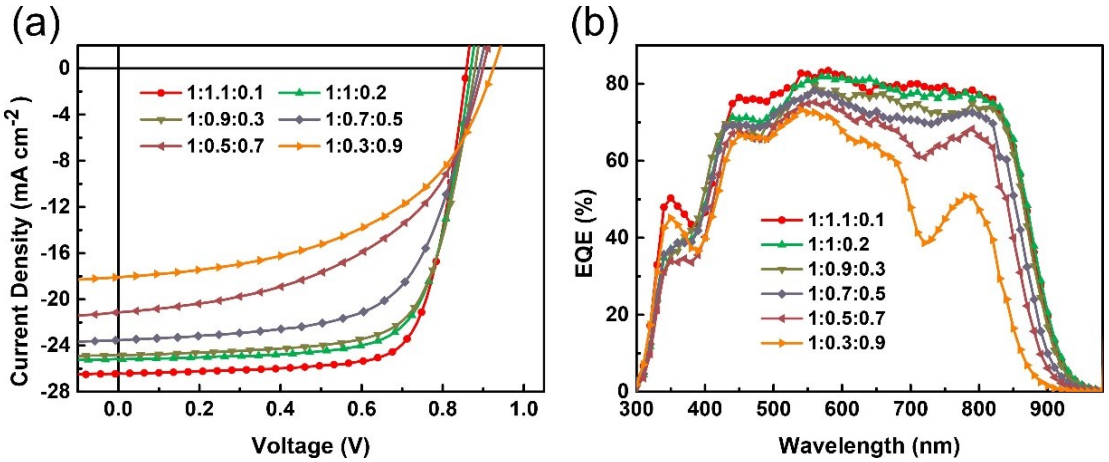

Figure S3. a) *J-V* curves and b) EQE spectra of the optimal ternary OSCs with different blend ratios.

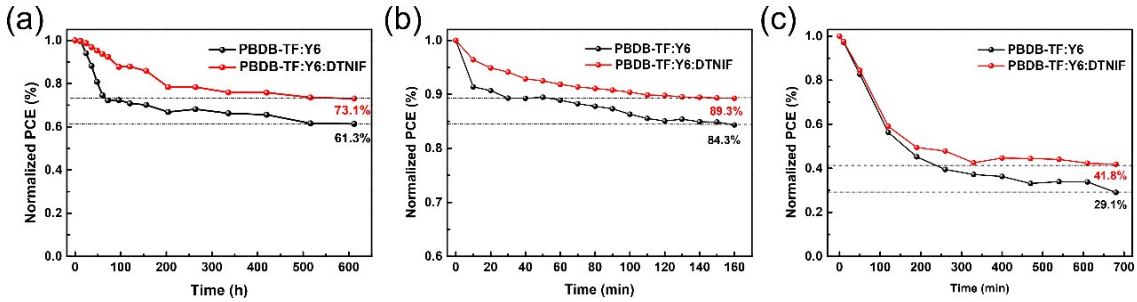

Figure S4. Normalized PCEs of the binary device based on PBDB-TF:Y6 and the ternary device based on PBDB-TF:Y6:DTNIF after storage in air (a), under light illumination (b), and under thermal aging at 80 ℃ (c).

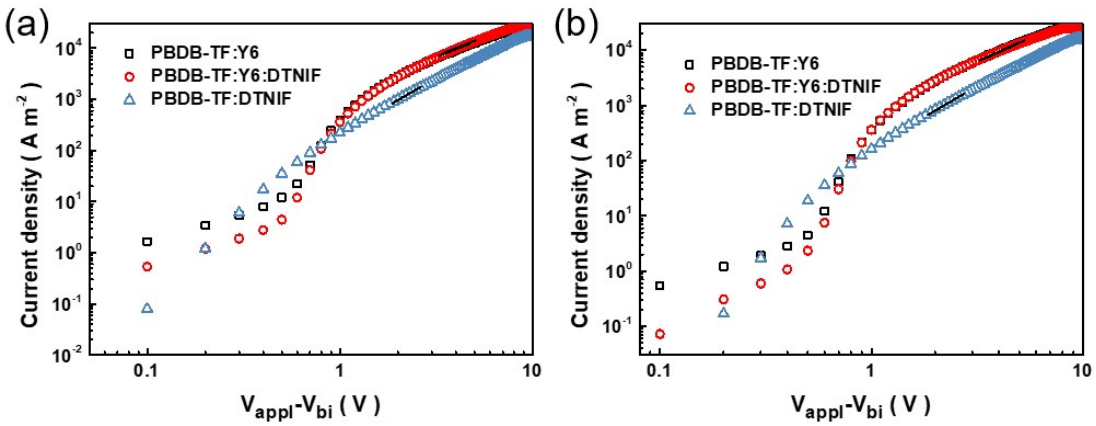

Figure S5. a) *J-V* curves for the a) hole-only and b) electron-only devices based on binary PBDB-TF:Y6, PBDB-TF:DTNIF and ternary PBDB-TF:Y6:DTNIF blends.

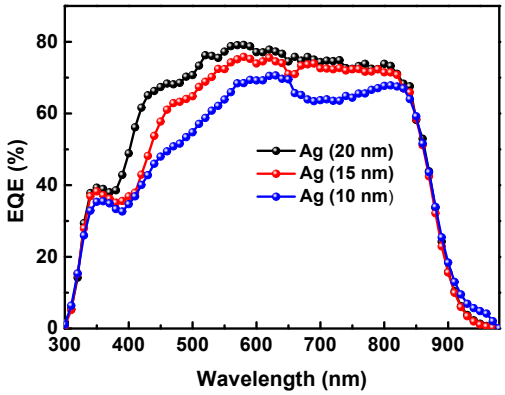

Figure S6. EQE spectra of the ternary semitransparent devices with different anode thicknesses (20, 15 and 10 nm).

检测数据/结果：
Data/Results of Test

1 Standard Test Condition (STC)： Total Irradiance： 1000 W/m^2
Temperature： 25.0 ℃
Spectral Distribution： AM1.5G

2. Measurement Data under STC

Test Times	I_{sc} (mA)	V_{oc} (V)	I_{MPP} (mA)	V_{MPP} (V)	P_{MPP} (mW)	*FF* (%)	η (%)
1	0.9078	0.8247	0.7934	0.6685	0.5304	70.85	13.43
2	0.9149	0.8248	0.7934	0.6681	0.5301	70.25	13.43
3	0.9199	0.8244	0.7934	0.6680	0.5300	69.89	13.42
Average Value	0.9142	0.8246	0.7934	0.6682	0.5302	70.33	13.43

Mismatch factor: 0.9959

3. I-V & P-V Characteristic Curves under STC

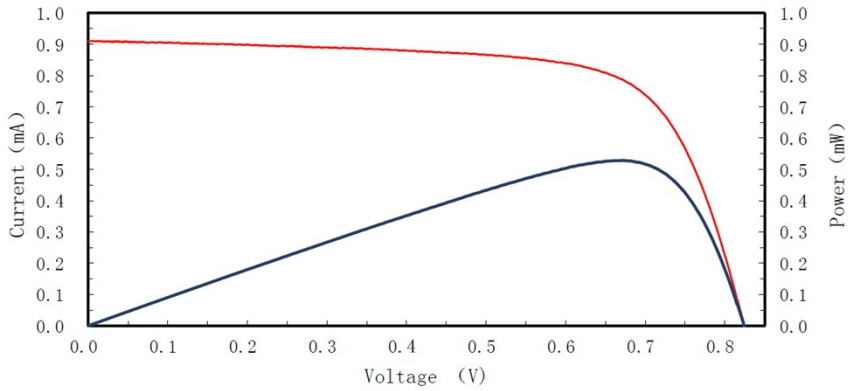

Figure 1. I-V and P-V characteristic curves of the measured sample under STC

Figure S7. Measurement and certification of the best-performance ternary semitransparent device based on PBDB-TF:Y6:DTNIF (15-nm Ag) from Fujian Metrology Institute (National PV Industry Measurement and Testing Center) in China.

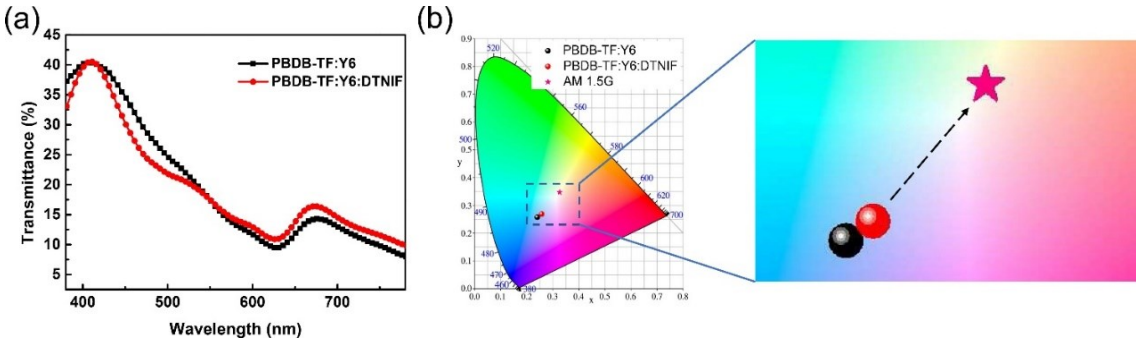

Figure S8. a) Visible transmittance spectra and b) the CIE 1931 color space of binary semitransparent device based on PBDB-TF:Y6 and the ternary semitransparent device based on PBDB-TF:Y6:DTNIF.

Table S1. Photovoltaic performance of the binary OSCs based on PBDB-TF:Y6 under different fabrication conditions.

PBDB-TF:Y6	V_{OC} [V]	J_{SC} [mA cm^{-2}]	FF [%]	PCE [%]	Thermal annealing
1.0:1.1	0.855	25.22	70.42	15.19	90 °C, 5 min
1.0:1.3	0.846	25.21	70.81	15.11	90 °C, 5 min
1.0:1.2	0.851	25.01	71.33	15.18	80 °C, 5 min
1.0:1.2	0.848	25.82	69.19	15.16	100 °C, 5 min
1.0:1.2	0.849	25.26	71.36	15.31	90 °C, 5 min
1.0:1.2	0.853	25.05	68.92	14.73	90 °C, 3 min
1.0:1.2	0.842	25.58	69.61	14.99	90 °C, 8 min

Table S2. Photovoltaic performance of the binary OSCs based on PBDB-TF:DTNIF under different fabrication conditions.

PBDB-TF:DTNIF	V_{OC} [V]	J_{SC} [mA cm^{-2}]	FF [%]	PCE [%]	Thermal Annealing
1:1.1	1.01	12.55	54.51	6.91	without
1:1.3	0.99	11.47	43.77	4.99	without
1:1.2	0.97	13.92	50.35	6.82	90 °C, 5 min
1:1.2	1.01	12.76	56.86	7.31	without

Table S3. Photovoltaic performance of the ternary OSCs based on PBDB-TF:Y6:DTNIF under different annealing conditions and different amounts of solvent additive.

PBDB-TF:Y6:DTNIF	V_{OC} [V]	J_{SC} [mA cm^{-2}]	FF [%]	PCE [%]	CN [%][a]	Thermal Annealing
1:1.1:0.1	0.860	26.22	72.25	16.28	0.5	80 °C, 5 min
1:1.1:0.1	0.856	26.70	70.73	16.16	0.5	100 °C, 5 min
1:1.1:0.1	0.859	25.64	72.69	16.02	0.3	90 °C, 5 min
1:1.1:0.1	0.860	25.67	72.23	15.94	0.8	90 °C, 5 min
1:1.1:0.1	0.858	26.40	73.80	16.73	0.5	90 °C, 5 min
1:1.1:0.1	0.861	26.52	72.16	16.48	0.5	90 °C, 3 min
1:1.1:0.1	0.857	26.07	71.07	15.88	0.5	90 °C, 8 min

[a] CN: 1-chloronaphthalene.

Table S4. Photovoltaic properties of OSCs based on the ternary PBDB-TF:Y6:DTNIF with different blend ratios.

PBDB-TF:Y6:DTNIF	V_{OC} [V]	J_{SC} [mA cm^{-2}]	FF [%]	PCE [%][a]	J_{cal} [mA cm^{-2}][b]
1.0:1.1:0.1	0.858	26.40	73.80	16.73 (16.48±0.13)	25.08
1.0:1.0:0.2	0.870	25.18	71.41	15.63 (15.50±0.11)	24.01
1.0:0.9:0.3	0.879	24.81	70.11	15.29 (15.21±0.07)	23.59
1.0:0.7:0.5	0.889	23.49	63.36	13.24 (13.16±0.07)	22.50
1.0:0.5:0.7	0.898	21.04	51.14	9.66 (9.59±0.11)	20.79
1.0:0.3:0.9	0.923	18.01	50.57	8.41 (8.39±0.06)	17.60

[a] Average PCEs were obtained from over 12 devices in parallel. [b] The J_{sc} values were calculated from the EQE curves.

Table S5. Parameters of the ordered structures.

PBDB-TF:Y6:DTNIF	π-π stacking		Lamellar stacking	
	d-spacing [Å][a]	CL [Å] (FWHM)[b]	*d*-spacing [Å][c]	CL [Å] (FWHM)
1.0:1.2:0	3.67	22.90 (0.247 Å^{-1})	20.93	54.03 (0.105 Å^{-1})
1.0:1.1:0.1	3.61	25.83 (0.219 Å^{-1})	20.72	69.61 (0.081 Å^{-1})

[a] (010) Diffraction peak along the q_z axis; [b] Coherent length (CL) estimated from the Scherrer equation (CL=2 π *k*/FWHM), in which *k* is the Scherrer factor and FWHM is the full-width at the half-maximum of the peak; [c] (100) Diffraction peak along the q_{xy} axis.

Table S6. Photovoltaic parameters of some representative STOSCs reported to date.

Active Layer	V_{OC} [V]	J_{SC} [mA cm^{-2}]	FF [%]	PCE [%]	AVT	Ref.
PTB7-Th:IEICO-4Cl	0.725	19.6	59.0	8.38	25.6	S4
PBDB-T:ITIC	0.88	13.8	59.8	7.3	25.2	S5
PTB7-Th:ATT-2	0.712	18.53	59	7.74	37	S6
PTB7-Th:BT-CIC	0.68	18.0	67.5	8.2	26	S7
PTB7-Th:IHIC	0.754	19.01	68.1	9.77	36	S8
PTB7-Th:$PC_{71}BM$	0.79	17.15	69.1	9.36	14.31	S9
PTB7-Th:PBT1-S:$PC_{71}BM$	0.83	15.6	70.8	9.2	20.0	S10
P3HT:ICBA	0.87	8.79	67.0	5.12	24.4	S11
PTB7-Th:IUIC	0.794	18.31	70.3	10.2	31	S12
J52:IEICO-4F:$PC_{71}BM$	0.690	19.04	67.2	8.83	15.8	S13
PTB7-Th:FNIC2	0.728	21.87	72.6	11.6	13.6	S14
P3TEA:FTTB-PDI4 (front) PTB7-Th:IEICS-4F (rear)	1.73	9.62	63	10.5	20	S15
PBDTTT-E-T:IEICO	0.81	14.4	66	7.9	23.8	S16
PM6:ID-4Cl	0.748	13.77	67.90	6.99	43.7	S17
PBN-S:IT-4F	0.878	15.48	65.5	8.88	34	S18

PTB7-Th:ITVfIC	0.742	17.54	63.11	8.21	26.4	S19
PTB7-Th:BDTThIT-4F:IEICO-4F	0.728	19.21	67.2	9.40	24.6	S20
PTB7-Th:$PC_{71}BM$	0.806	14.59	72.4	8.52	26.2	S21
PIDT-phanQ:$PC_{61}BM$ (front) PIDT-phanQ:$PC_{71}BM$ (rear)	1.63	5.23	68.94	7.4	40	S22
PM6:Y6	0.852	20.35	71.36	12.37	18.6	S23
PTB7-Th:IEICO-4F	0.707	20.27	67.4	10.03	34.2	S24
J71:PTB7-Th:HIC	0.76	21.08	58.05	9.37	21.4	S25
PBDB-T-2F:Y6	0.825	21.56	72.41	12.88	25.6	S26
PBDB-TF:Y6:DTNIF	0.857	23.61	71.64	14.50	19.78	This work
PBDB-TF:Y6:DTNIF	0.847	22.71	70.16	13.49	22.58	This work
PBDB-TF:Y6:DTNIF	0.844	20.56	69.93	12.14	25.89	This work

References

[S1] M. Zhang, Y. Ma, Q. Zheng, *Front. Chem.,* 2018, **6**, 427.

[S2] P. W. M. Blom, M. J. M. de Jong, M. G. van Munster, *Phys. Rev. B*, 1997, **55**, R656.

[S3] G. G. Malliaras, J. R. Salem, P. J. Brock, C. Scott, *Phys. Rev. B*, 1998, **58**, R13411.

[S4] Y. Cui, C. Yang, H. Yao, J. Zhu, Y. Wang, G. Jia, F. Gao, J. Hou, *Adv. Mater.*, 2017, **29***,* 1703080.

[S5] M. B. Upama, M. Wright, N. K. Elumalai, M. A. Mahmud, D. Wang, C. Xu, A. Uddin, *ACS Photonics*, 2017, **4**, 2327.

[S6] F. Liu, Z. Zhou, C. Zhang, J. Zhang, Q. Hu, T. Vergote, F. Liu, T. P. Russell, X. Zhu, *Adv. Mater.*, 2017, **29***,* 1606574.

[S7] Y. Li, J. D. Lin, X. Che, Y. Qu, F. Liu, L. S. Liao, S. R. Forrest, *J. Am. Chem. Soc.*, 2017, **139**, 17114.

[S8] W. Wang, C. Yan, T. K. Lau, J. Wang, K. Liu, Y. Fan, X. Lu, X. Zhan, *Adv. Mater.*, 2017, **29***,* 1701308.

[S9] P. Shen, M. Yao, J. Liu, Y. Long, W. Guo, L. Shen, *J. Mater. Chem. A*, 2019, **7**, 4102.

[S10] Y. Xie, L. Huo, B. Fan, H. Fu, Y. Cai, L. Zhang, Z. Li, Y. Wang, W. Ma, Y. Chen, Y. Sun, *Adv. Funct. Mater.*, 2018, **28***,* 1800627.

[S11] W. Yu, X. Jia, M. Yao, L. Zhu, Y. Long, L. Shen, *Phys. Chem. Chem. Phys.*, 2015, **17**, 23732.

[S12] B. Jia, S. Dai, Z. Ke, C. Yan, W. Ma, X. Zhan, *Chem. Mater.*, 2017, **30**, 239.

[S13] H. Shi, R. Xia, G. Zhang, H.-L. Yip, Y. Cao, *Adv. Energy Mater.*, 2019, **9**, 1803438.

[S14] J. Wang, J. Zhang, Y. Xiao, T. Xiao, R. Zhu, C. Yan, Y. Fu, G. Lu, X. Lu, S. R. Marder, X. Zhan, *J. Am. Chem. Soc.*, 2018, **140**, 9140.

[S15] S. Chen, H. Yao, B. Hu, G. Zhang, L. Arunagiri, L.-K. Ma, J. Huang, J. Zhang, Z. Zhu, F. Bai, W. Ma, H. Yan, *Adv. Energy Mater.*, 2018, **8**, 1800529.

[S16] C. Sun, R. Xia, H. Shi, H. Yao, X. Liu, J. Hou, F. Huang, H.-L. Yip, Y. Cao, *Joule*, 2018, **2**, 1816.

[S17] X. Li, H. Meng, F. Shen, D. Su, S. Huo, J. Shan, J. Huang, C. Zhan, *Dyes Pigm.*, 2019, **166**, 196.

[S18] Y. Wu, H. Yang, Y. Zou, Y. Dong, J. Yuan, C. Cui, Y. Li, *Energy Environ. Sci.*, 2019, **12**, 675.

[S19] H. Huang, X. Li, L. Zhong, B. Qiu, Y. Yang, Z.-G. Zhang, Z. Zhang, Y. Li, *J. Mater. Chem. A*, 2018, **6**, 4670.

[S20] Z. Hu, J. Wang, Z. Wang, W. Gao, Q. An, M. Zhang, X. Ma, J. Wang, J. Miao, C. Yang, F. Zhang, *Nano Energy*, 2019, **55**, 424.

[S21] B. Dudem, J. W. Jung, J. S. Yu, *J. Mater. Chem. A*, 2018, **6**, 14769.

[S22] C.-Y. Chang, L. Zuo, H.-L. Yip, C.-Z. Li, Y. Li, C.-S. Hsu, Y.-J. Cheng, H. Chen, A. K. Y. Jen, *Adv. Energy Mater.*, 2014, **4**, 1301645.

[S23] Z. Hu, Z. Wang, Q. An, F. Zhang, *Sci. Bull.*, 2020, **65**, 131.

[S24] Y. Liu, P. Cheng, T. Li, R. Wang, Y. Li, S. Y. Chang, Y. Zhu, H. W. Cheng, K. H. Wei, X. Zhan, B. Sun, Y. Yang, *ACS Nano*, 2019, **13**, 1071.

[S25] J. Zhang, G. Xu, F. Tao, G. Zeng, M. Zhang, Y. Yang, Y. Li, Y. Li, *Adv. Mater.*, 2019, **31**, 1807159.

[S26] Y. Bai, C. Zhao, X. Chen, S. Zhang, S. Zhang, T. Hayat, A. Alsaedi, Z. A. Tan, J. Hou, Y. Li, *J. Mater. Chem. A*, 2019, **7**, 15887.